Monograph:
Edwards, J.B. and Twemlow, J.K. (1982) Wide-Beam Sensors for Controlling Dual-Delay Systems. Research Report. ACSE Report 197 . Department of Control Engineering, University of Sheffield, Mappin Street, Sheffield

WIDE-BEAM SENSORS FOR CONTROLLING DUAL-DELAY SYSTEMS

by

J.B. Edwards and J.K. Twemlow

Department of Control Engineering,
University of Sheffield,
Mappin Street, Sheffield S1 3JD.

Research Report No. 197

September 1982

A paper submitted to the Institution of Electrical Engineers for publication in the Proceedings.

SYNOPSIS

An important class of dual delay feedback systems of open-loop trasnfer-function $G(s) = k \exp(-Xs)/\{1 - \exp(-Ws)\}$ is shown to be unstable if ratio X/W is noninteger. By means of z-transform techniques it is shown that, by using a feedback transducer that senses over a substantial distance either side its central axis, closed-loop stability may be restored. Such transducers, here termed wide-beam sensors, include transmission, backscatter and natural radiation types as well as electromechanical conveyor-belt weighers etc. The paper demonstrates that designing transducers for very narrow beams may not be desirable from the overall system viewpoint.

WIDE-BEAM SENSORS FOR CONTROLLING DUAL-DELAY SYSTEMS

J.B. Edwards and J.K. Twemlow

1. List of Symbols and Abbreviations

B	Width of radiation beam received by sensor crystal
Dual-Delay System	System having configuration of Fig. 1
ε	Additional sensor offset from position n W (equation 3)
G(s)	Transfer-function of dual-delay system with pencil-beam sensor
$G_p(z)$	z-transfer function of dual-delay system with pencil·beam sensor
$G_s(z)$	z-transfer-function of uniform wide-beam sensor
$G_{ps}(z)$	z-transfer-function of combined process and wide-beam sensor
H(s)	Low-pass filter representing floor degradation
k	Controller gain
n	Integer (=X/W in Section 3.1 and = $(X-\varepsilon)/W$ elsewhere)
Pencil beam	Infinitessimally narrow beam of received radiation
q	Integer = $B/2\varepsilon$
r	Integer = W/ε
s	Laplace variable
y	Output of process proper
y'	Sensed output
y^*	y' sampled at distance intervals ε
$y^\dagger$	y^* processed by zero-order hold device
W	Process delay distance
Wide beam	Radiation beam (received by transducer) having a finite width
x	Distance travelled
X	Sensor delay distance (measured to beam centre)
z	Complex, independent variable in z-transforms (=$e^{s\varepsilon}$)
ω	Angular frequency in radians p.u. distance

2. INTRODUCTION

An important class of mechanical processes involves two transport delays arranged in the configuration of Fig. 1 in which y denotes the process output, y' its measured value, y_r the desired value of y, u the control, W and X the process and measurement delay distances respectively and s is a complex frequency measured in radians per unit distance. Controllers are usually of the simple proportional type and are represented in Fig. 1 by the static gain k. The open-loop transfer-function G(s) of this type of process is therefore given by

$$G(s) = \frac{k \exp(-Xs)}{\{1 - \exp(-Ws)\}} \qquad (1)$$

The denominator term $\{1 - \exp(-Ws)\}$ arises quite generally[(1),(2),(3)] in modelling the basic, constant-speed, manoeuvring dynamics of excavating, mining and earth-moving machines which cut or clear the floor upon which they subsequently travel. Such a machine is illustrated diagramatically in Fig. 2. The machine-height sensor is very frequently of a natural- or back-scattered-radiation type and situated well away from the leading end of the machine to avoid risk of damage to the sensor. Strata above and/or below the excavation generally occurs in fairly uniform parallel layers of differing mineral content and microscopic structure. Each layer therefore generates its own characteristic radiation spectrum so that the height of the machine within the strata pattern can generally be computed from the total natural radiation received at the detector. Natural gamma sensors[(4)] operate on this principle. Backscatter gauges[(5)] rely on the differing degrees of scatter produced by the strata layers on an artificial radiation beam produced by a radio-active isotope located in the sensor but shielded from the detector.

Sensor action is modelled, at its simplest, by the transport delay exp(-Xs), assuming the height measurement to be made at a point and, indeed, considerable effort is generally devoted to obtaining as narrow a sensor beam-width as possible. This is achieved through beam collimation by recessing the detecting crystal within a tube of shielding material, as indicated in Fig. 2. Severe collimation (resulting from either too-deep a tube or too-small a crystal area) reduces the strength of the gamma radiation received, however, so increasing the randomness of the height-signal obtained with a given filter time-constant, (or demanding an excessive filter lag for a given standard-deviation of output signal). Narrowing the beamwidth to a pencil certainly simplifies system analysis, permitting the use of transfer-function G(s) (perhaps augmented by sensor-and actuator-lags) in system studies but does not necessarily aid system behaviour, as will be revealed in the paper.

For control systems design, the only attempts hitherto to include random radiation effects[6] have involved the use of pseudorandom-binary or near-Poisson sequence generators whose average (clock) frequency is modulated by a varying point-measurement of roof (or floor) height. In control studies, no attempt has been made to examine the effect of the spatial distribution of the received radiation beam. Detailed modelling[4] of radiation sensors is extremely complicated, requiring expensive simulation that involves solution of a Boltzman transport equation by Monte Carlo methods. Even for static tests (i.e. with a sensor held stationary) the tracking of numerous individual quanta throughout the gamma field is strictly necessary. Their paths involve many random collisions and backscatter operations and the field ultimately supplying radiation to the sensing crystal therefore covers a range outside the simple umbral- and penumbral-cones indicated in Fig. 2. Once the sensor moves, the gamma- transport process is further complicated, even with constant, homogeneous roof-(or floor-) strata. A wider gamma field must now be monitored because the fringes of the field clearly make different contributions to the received radiation level to those in the stationary situation. For analytical ...ies of the idealised process, G(s), as defined by equation (1), may clearly be treated as a continuous linear system. To augment G(s) with even the simplest wide-beam sensor model would, however, eliminate the system linearity because no linear continuous transfer-function could represent the wide-beam effect. Quite apart from the complexities mentioned above, the beam-width must be finite to prevent the sensor from seeing ahead of the excavation and producing consequent causality problems. Continuous linear transfer-function approximations of a radiation beam of significant width are therefore precluded.

Fortunately, the dual-delay system G(s) can also be regarded as a discrete system and, as shown in Section 3, readily yields to analysis by z-transform methods. A finite sensor beam profile can also be described as a linear discrete process thus allowing the composite system, G(s) + sensor, to be analysed. This is demonstrated in Section 4, producing interesting predictions for the potential benefits of wide-beam sensors. Simulation is used to validate the z-domain findings.

3. THE DUAL-DELAY SYSTEM ALONE

3.1 Integer Delay Ratios

Setting the ratio

$$X/W = n, \ n=1,2, \text{ etc.} \qquad (2)$$

produces inverse Nyquist loci $G^{-1}(j\omega)$ of the forms shown in Fig. 3. As integer n is increased the locus shapes increase in complexity but all share the property that the locus repeats itself precisely as frequency ω changes through an increment $2\pi/W$, describing n counterclockwise revolutions around a portion of the negative real axis in the process. Thus, if N is an integer of infinite proportions, the number of such orbits traced as ω describes the range $-N\pi/W \leq \omega \leq N\pi/W$ (i.e. as s traverses the imaginary axis of the s-plane) will be nN. This equals the number of clockwise infinite encirclements made by $G^{-1}(s)$ $\{= k^{-1}R \exp (X N\pi W^{-1} j \sin \theta), R \to \infty\}$ as s completes the D-contour, at radius $N\pi/W$, around the unstable half s-plane. A region of stability, indicated by the hatching in the examples of Fig. 3, therefore occurs in which to site the critical -1 + j o point by suitable choice of controller gain k. The critical values of k are clearly 2.0 and 1.0 respectively for the cases of n=1 and 2 illustrated.

3.2 Noninteger Delay Ratios

Once the delay ratio X/W becomes noninteger, e.g. if

$$X = nW + \varepsilon, \quad W > \varepsilon > 0, \; n=1,2,3 \text{ etc.} \tag{3}$$

then $G^{-1}(s)$ may be written:

$$G^{-1}(s) = \left[k^{-1}\{1 - \exp(-Ws)\} \exp(nWs)\right] \exp(\varepsilon s) \tag{4}$$

The square-bracketed term clearly generates a locus identical to that produced in the case of an integer delay ratio of value n, but the additional modulating term exp $(\varepsilon j\omega)$ now causes a progressive counterclockwise rotation of this pattern in the G^{-1} - plane as indicated in Fig. 4. The overall locus shape therefore no longer repeats itself precisely every frequency increment $2\pi/W$ and the previous region of stability is progressively eroded away to zero with each traverse of the basic pattern. Stability by adjustment of k therefore cannot now be achieved. [Compensation by means of a rational cascaded filter is also ineffective for although such a network can move the critical point towards the origin as ω increases, it must inevitably loose the race to the origin as its speed of approach falls in that vicinity]. Dual-delay systems of this type therefore present a significant stability problem. Before considering its solution by wide-beam sensors, however, we first confirm the findings of Sections 3.2 by means of the z-transform method.

3.3 z-Transform Analysis

For this analysis we again consider the more general situation of a noninteger ratio X/W, i.e. we set

$$X = nW + \varepsilon, \quad W > \varepsilon > 0, \; n=1,2,3, \text{ etc.} \tag{5}$$

as in Section 3.2, but we impose the minor restriction that

$$W/\varepsilon = r \quad , \quad r = 2,3,4 \text{ etc.} \tag{6}$$

The system may be represented by the block diagram of Fig. 5.

Now because unforced transitions in the variables of this system will take place only at intervals, ε, the natural vibrations of the system will be unaffected by the introduction of a cascaded sampler and zero-order hold device indicated in Fig. 6. The stability of these two equivalent systems may therefore be determined from observation of the sequence $y^{\dagger}$ appearing at the output of the zero-order-hold. Setting $e^{s\varepsilon} = z$ and using standard tables of z-transforms, the open-loop z-transfer function of the process is readily shown to be

$$G_p(z) = \frac{k\, z^{-1}\, z^{-nr} z(1-z^{-1})}{(1-z^{-r})(z-1)} = \frac{k}{(z^r-1)z^{(nr-r+1)}} \tag{7}$$

$G_p(z)$ clearly has nr-r+1 poles clustered at the origin of the z-plane and r poles arranged uniformly around the unit circle. For r-even, there will therefore be nr + 1, (i.e. an odd number), of poles on or within the unit circle so that the root locus lies along the real axis everywhere outside and nowhere inside the circle indicating complete instability no matter what the value of k. This result clearly accords with the continuous system analysis of Section 3.2. Instability for any $k > o$ in the case of r-odd is readily argued on the basis of angles of departure of the locus branches from the peripheral poles. For the case of n=2, r=3 for instance, the departure from pole A in Fig. 7 will clearly take place at $(180 - 90 - 4 \times 120 - 150)^\circ \equiv 180^\circ$, i.e. immediately into the unstable region $|z| > 1.0$ once k exceeds zero. The z-transform method thus confirms continuous frequency domain analysis and is therefore a useful tool for examining dual-delay systems in which X/W is noninteger, provided the discrepancy ε is such that the ratio $r = W/\varepsilon$ is integer. A transient response computed for the case n=2, r=2 i.e. $X = 5\varepsilon$, $W = 2\varepsilon$ is given in Fig. 8 confirming the expected instability of this system. The instability of many other cases has also been confirmed.

The result is serious in its practical implications since mechanical constraints and positional tolerances may not allow X/W to be set to an integer number in practice and furthermore may not be precisely constant (due to variable boom tilt for instance in Fig. 2).

4. THE EFFECT OF SENSOR BEAM-WIDTH

Instead of a sensor of infinitessimal beam-width, consider now a symmetrical sensor beam whose centre is again delayed by distance $X\{= (nr + 1)\varepsilon\}$ as before but of finite width B where

$$B = 2\,q\,\varepsilon \tag{8}$$

where

$$q \leq nr + 1 \tag{9}$$

i.e. where

$$B/2 \leq X \tag{10}$$

as required by causality. In this initial investigation we assume a uniform beam so that the sensor's response to a unit impulse in y is a rectangular pulse of unit height and having a width, B, centred on the initiating impulse as illustrated in Fig. 9. The response can be regarded as a positive unit step function at $x = -q\varepsilon$ plus a negative unit step at $x = (q+1)\varepsilon$ (assuming the impulse to occur at $x = 0$). The z-transfer function of the sensor is therefore

$$G_s(z) = \frac{z}{(z-1)}\,z^{q} - \frac{z}{(z-1)}\,z^{-(q+1)} = \frac{z(z^{q} - z^{-(q+1)})}{(z-1)} \tag{11}$$

(Alternatively $G_s(z)$ may be derived by summation of the train of the $2q + 1$ impulses occuring between $x = -q\varepsilon$ and $x = +q\varepsilon$ that are produced on sampling the sensor output, Laplace transforming and setting $z = e^{s\varepsilon}$). With the inclusion of such a sensor, variable transitions throughout the entire process will still occur discretely and only at intervals ε so that the composite process + sensor system will have an open-loop z-transfer function $G_{ps}(z)$ given by

$$G_{ps}(z) = G_p(z)\ G_s(z) \tag{12}$$

Relationships (12) is, of course, not true for cascaded subsystems generally in the absence of interposed samplers. Such samplers can be conceptually introduced quite freely in the case of the systems studied here however, because of their integer-delay nature. From equations (7) (11) and (12) therefore we obtain

$$G_{ps}(z) = \frac{k(z^{2q+1} - 1)}{z^{(nr-r+q+1)}(z-1)(z^r-1)} \tag{13}$$

In the special case n = 2, r = 2, q = 1 therefore:

$$G_{ps}(z) = k\ (z^3 - 1)/\ \{z^4(z-1)(z^2 - 1)\} \tag{14}$$

This clearly yields the pole/zero pattern shown in Fig. 10 from which it is immediately deduced that the real axis is occupied by the root locus only within the unit circle. The closed-loop roots ultimately leave the stability region $|z| < 1.0$ as k is increased at the complex points shown in Fig. 10 but scope for stabilization by appropriate gain setting is now an obvious possibility (not available in the case of the pencil beam sensor of Section 3). The hitherto unstable system of Fig. 8 is thus stabilised by introduction of the wide-beam sensor as confirmed by the computed transient response shown in Fig. 11.

5. Discussion and Conclusions

Designers of sensors for the detection of natural, transmitted or backscattered radiation aim generally for as narrow a beam-width as possible, subject to a minimum acceptable signal-strength dictated by noise considerations. The paper has demonstrated that a pencil beam used in the conventional proportional control of an important class of dual-delay systems, $G_s(s) = k\ \exp(-Xs)/\{1 - \exp(-Ws)\}$, will produce instability of the beam is not located precisely to produce a measurement delay, X, equal to an integer number, n, of process delays, W. Mechanical constraints, tolerances and variations in W and X may render the relationship $X = nW$ unattainable in practice, introducing an unwanted additional displacement ε such that $X = nW + \varepsilon$ in this situation. The prediction has been made using continuous frequency domain analysis and also, by treating the process as a discrete system, using the z-transform method. Some assessment of the problems that might arise in real life is appropriate however:

The predicted oscillations are expected to occur at a cyclic frequency of $0.5\ \varepsilon^{-1}$ (see Fig. 8) and, in the type of application envisaged, the rectangular humps and hollows of width ε may reasonably be expected to be destroyed and so go undetected by the process if ε is relatively small compared to W . The discrepancy between theoretical and practical expectations arises, of course, in the original choice of mathematical process model, which like all mathematical models of real processes is approximate to some extent. Additional cascaded rational transfer-functions due to sensor and actuator lags do not alter the theoretical predictions significantly (as has already been argued in Section 3.2). In the case of earthmoving and mining applications, degradation of the floor between being cut and the process settling thereon does affect the high-frequency performance however, since, at its simplest such a process if linear, modifies G_s to the form

$$G_s(s) = k \exp(-Xs) / \{1 - H(s) \exp(-Ws)\} \qquad (15)$$

where H(s) is a form of low-pass filtering process which retains the assumed value of unity until a critical high frequency is reached. Thereupon the floor undulations shear off. The validity of prediction therefore depends on the relative size of the unwanted delay distance ε and situations readily occur where this may amount to 10 cm or considerably more. The problem would therefore appear to be one or more than academic interest in such applications.

z-transform analysis allows wide sensor beams of simple analytical profile to be incorporated within the stability analysis. A simple rectangular profiled beam of significant width (= W in a particular case considered) has been shown to stabilise a process that would be otherwise unstable (e.g. where $\varepsilon = W/2$) indicating that broad-beam sensors may have a potentially important role in the control of these systems. A partial explanation of the extra stabilising power of a broad-beam sensor (compared to a rational filter) is that, having a near-symmetrical two-sided impulse response (about the nominal delay distance X) it does not introduce any significant phase-shift and thus causes the critical point of the inverse Nyquist diagram to move towards the origin along the real axis as ω increases rather than via a complex path. Intersection with the $G_s^{-1}(j\omega)$ locus is thus postponed. A full explanation in terms of the continuous frequency domain is complicated however, because of the necessarily nonlinear nature of the sensor's response.

In the z-transform approach attention was necessarily restricted to beams that involve only an integer, number, q, of error distances ε, where $r\,\varepsilon = W$, r also being an integer. There therefore exists the possibility of instability in practice if these conditions are contravened. Although this situation has not been generally analysed, simulation of particular cases, e.g. X=2.5W, B=0.95W, (taking care to ensure an adequate simulation time step for observation of the possible unwanted higher frequency modes) yields step responses typified by Fig. 12. Clearly the system remains substantially stable apart from a very slowly growing spiky instability that would clearly be ironed out in the practical situation by the smoothing effects of H(s) discussed earlier in this section.

Differential delay systems can frequently be compensated and adequately controlled by the use of Smith predictors[7] but a fairly precise knowledge of the system delay is often required a priori. At first sight the use of such predictors would therefore seem to favour narrow beam sensors. Little investigation of Smith predictors in dual-delay systems has been undertaken however, and where the additional process delay may also be the subject of uncertainty the widebeam sensor may well provide a more attractive alternative, particularly as it avoids the need for digital storage in a controller.

Finally it is worth noting that radiation sensors of various types are finding increasing use in process industries for thickness, density, composition and quantity control. They are not the only type of transducer that possess the wide-beam averaging characteristic however. Electromechanical belt weighers, for instance, make their measurements over a significant distance either side the central axis of the transducer. The two-sided characteristic of the response of such devices would therefore appear to be well worth future investigation as a potential control systems stabiliser. Dual-delay systems would appear to merit further investigation in their own right in view of the unstable modes they can readily generate.

6. REFERENCES

(1) Nicholson, H. (Ed): 'Modelling dynamical systems, Vol. II', Peter Peregrinus I.E.E. Control Engineering Series 13, 1981, pp. 178-233.

(2) Edwards, J.B. and Twemlow, J.K.P.: 'Mathematical modelling of the In-Seam Miner', Report to Mining Research and Development Est., Jan. 1982, 12 pp.

(3) 'The N.C.B./Dosco In Seam Miner', Major Development Committee Information Bulletin No. TG/79/1, Mining Research and Development Establishment (N.C.B.) 1979, 19 pp.

(4) Wykes, J.S., Adsley, I., Cooper, L.R. and Croke, G.M. 'Natural gamma radiation : A steering guide in coal seams', N.C.B., M.R.D.E., Internal report 1981: to be published.

(5) Cooper, L.R.: 'Gamma-ray backscatter gauges for measuring coal thickness on mechanised coal faces', Proc. of I.E.E. International Conference on Industrial Measurement and Control by Radiation Techniques', Guildford, 1972, I.E.E. Conf. Pub. No. 84, pp. 89-93.

(6) Edwards, J.B. and Addison, G.J.: 'The nucleonic coal sensor as an element of a control system for automatic steering of a coal cutter', ibid., pp. 20-29.

(7) Marshal, J.E.: 'Control of time delay systems', Peter Peregrinus, I.E.E. Control Engineering Series 10, 1979.

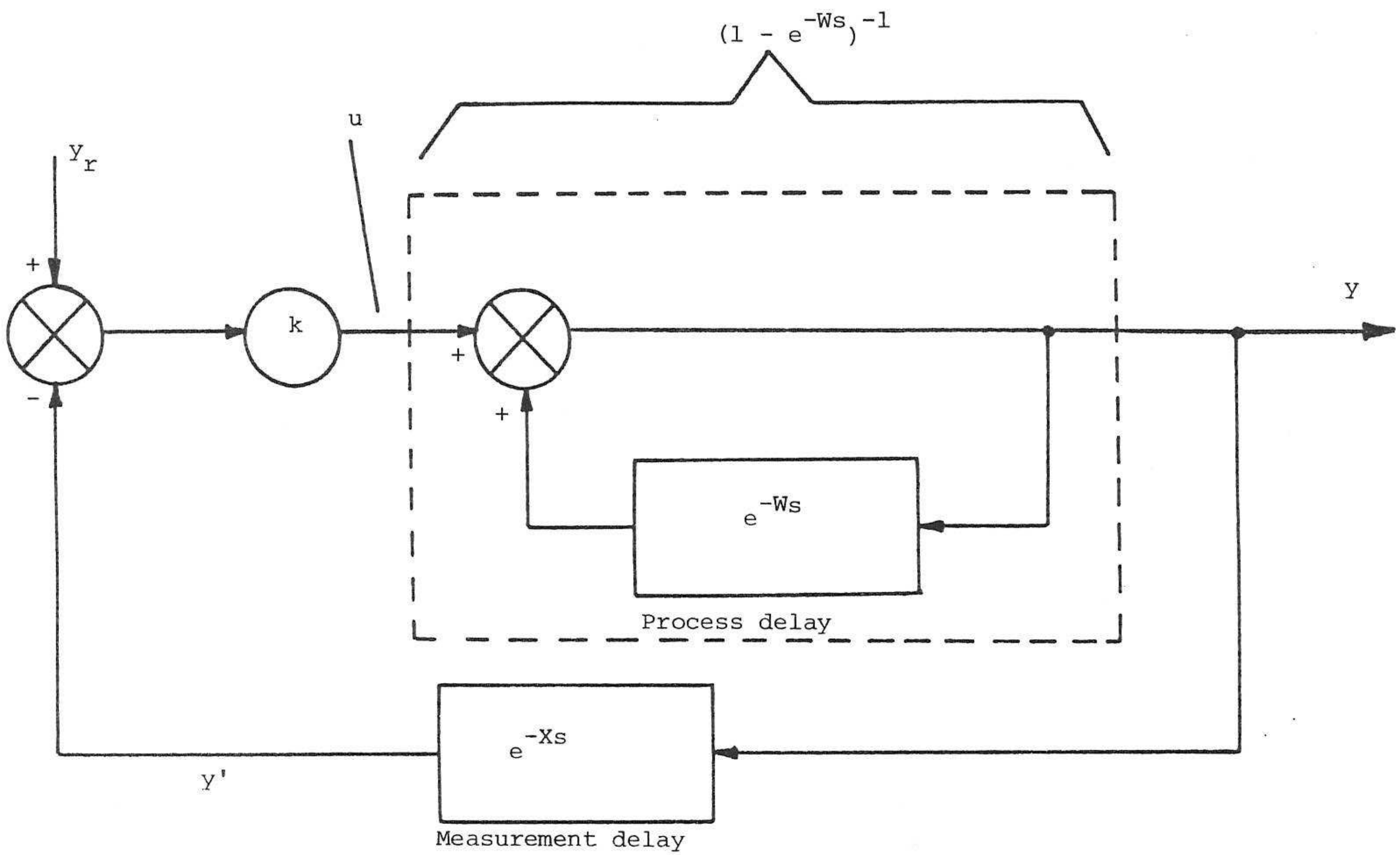

Fig. 1 Block diagram representation of dual delay system

Fig. 2 Tunnelling Machine

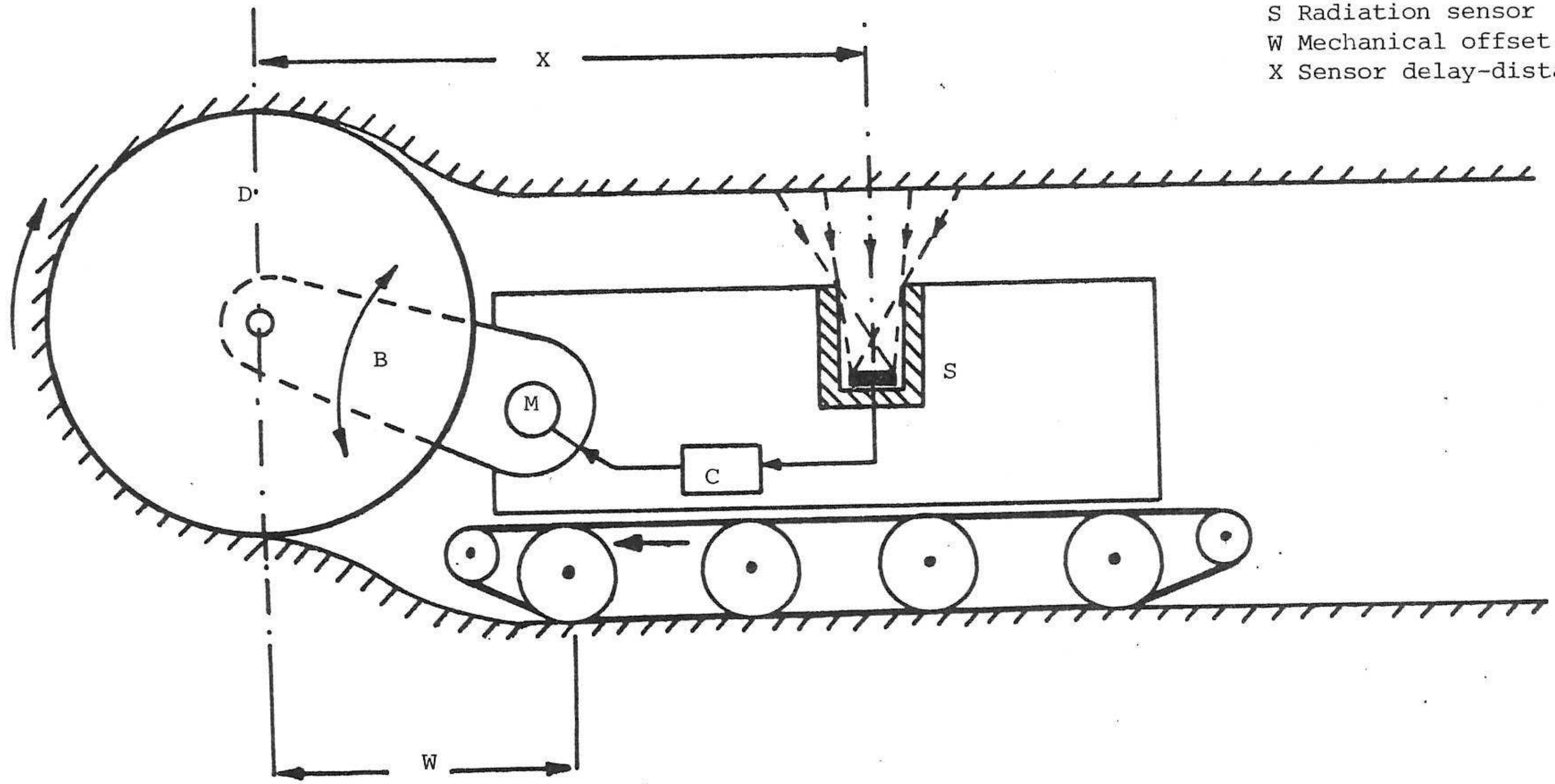

Key

B Steering boom
C Controller
D Excavating drum
M Boom-tilting motor
S Radiation sensor
W Mechanical offset distance
X Sensor delay-distance

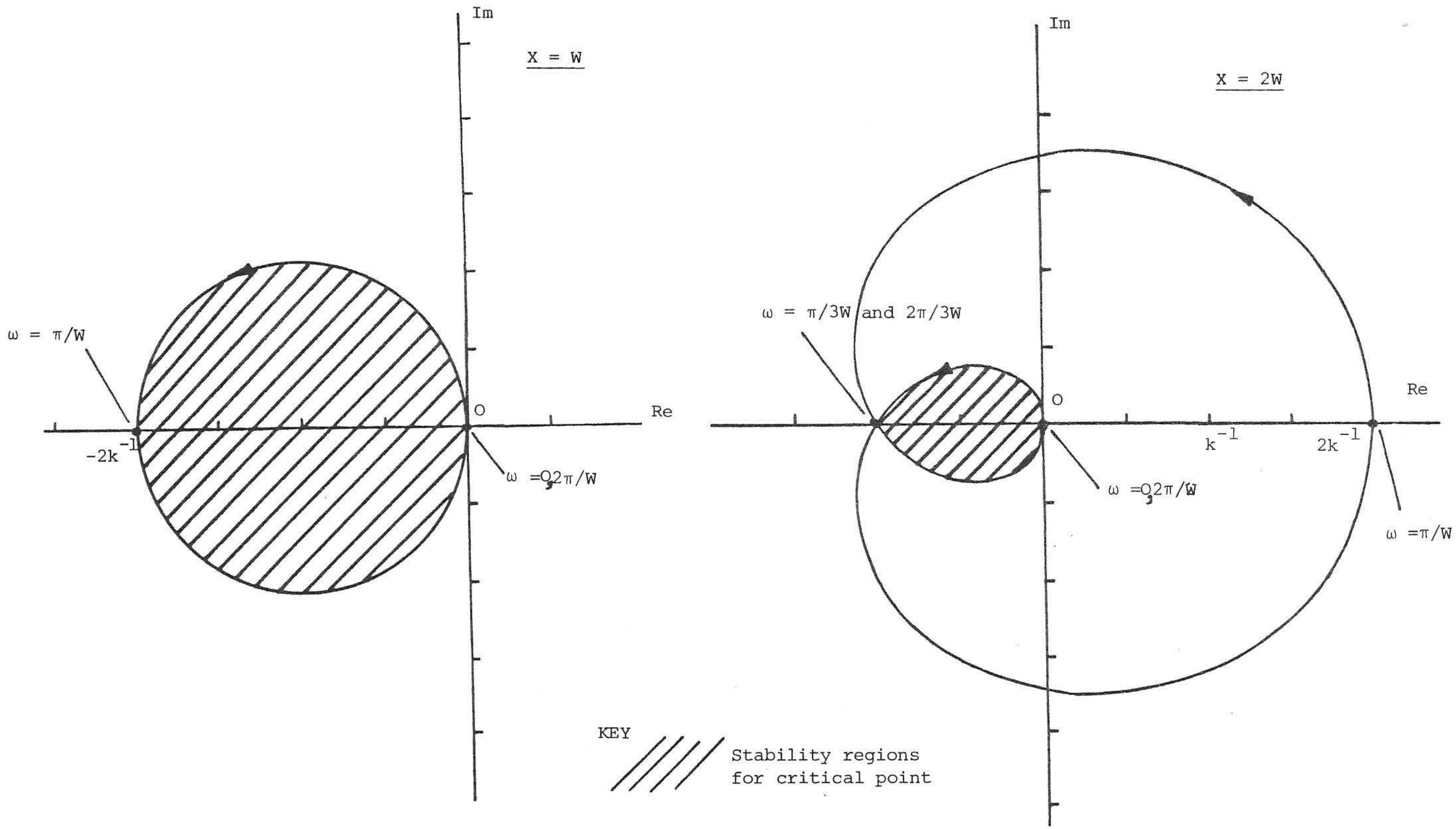

Fig. 3 Inverse Nyquist loci for $G_s(j\omega)$ having integer delay ratios X/W

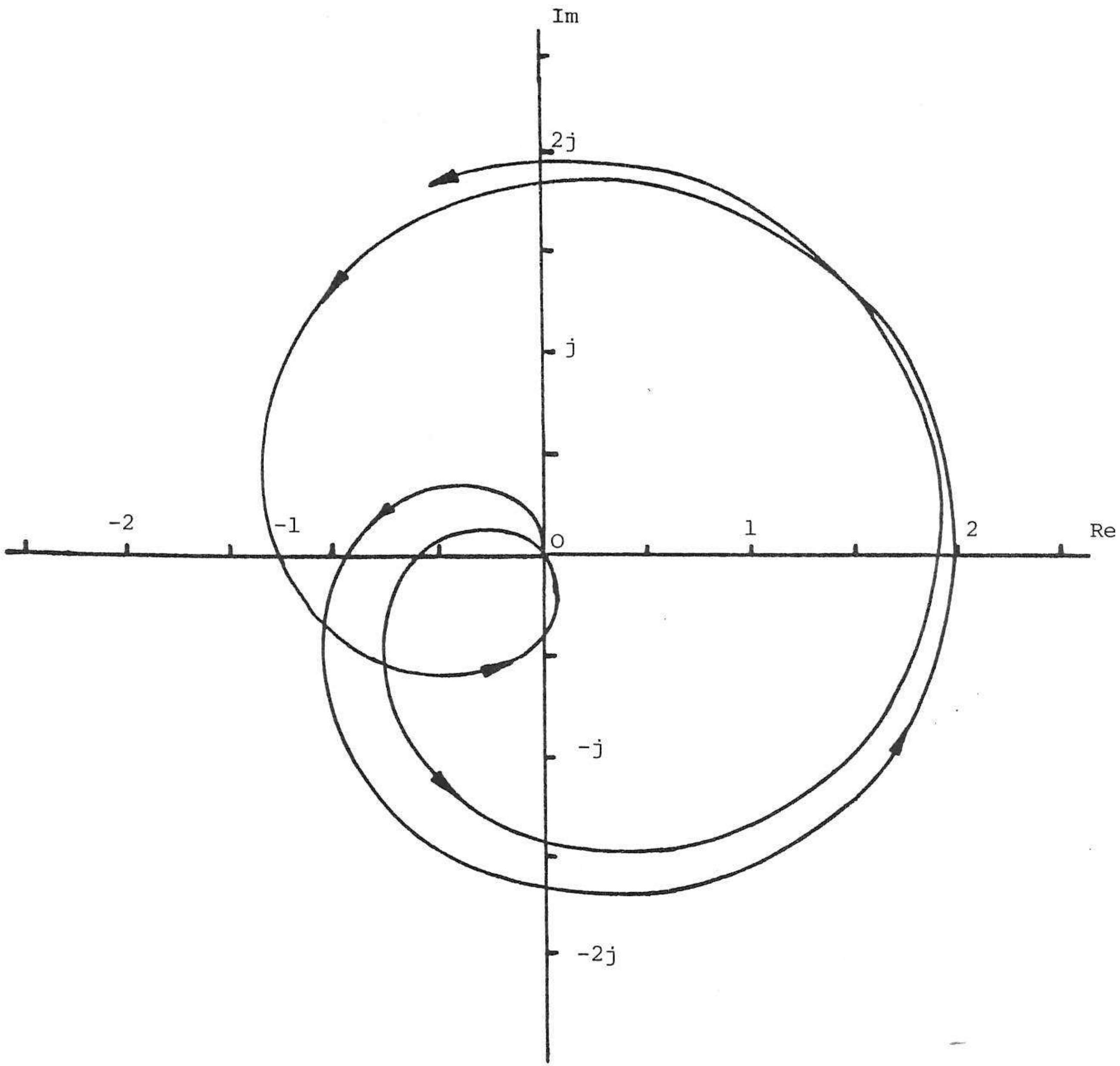

Fig. 4 Inverse Nyquist locus for X/W = 2.1 showing erosion of stability zone (k = 1.0)

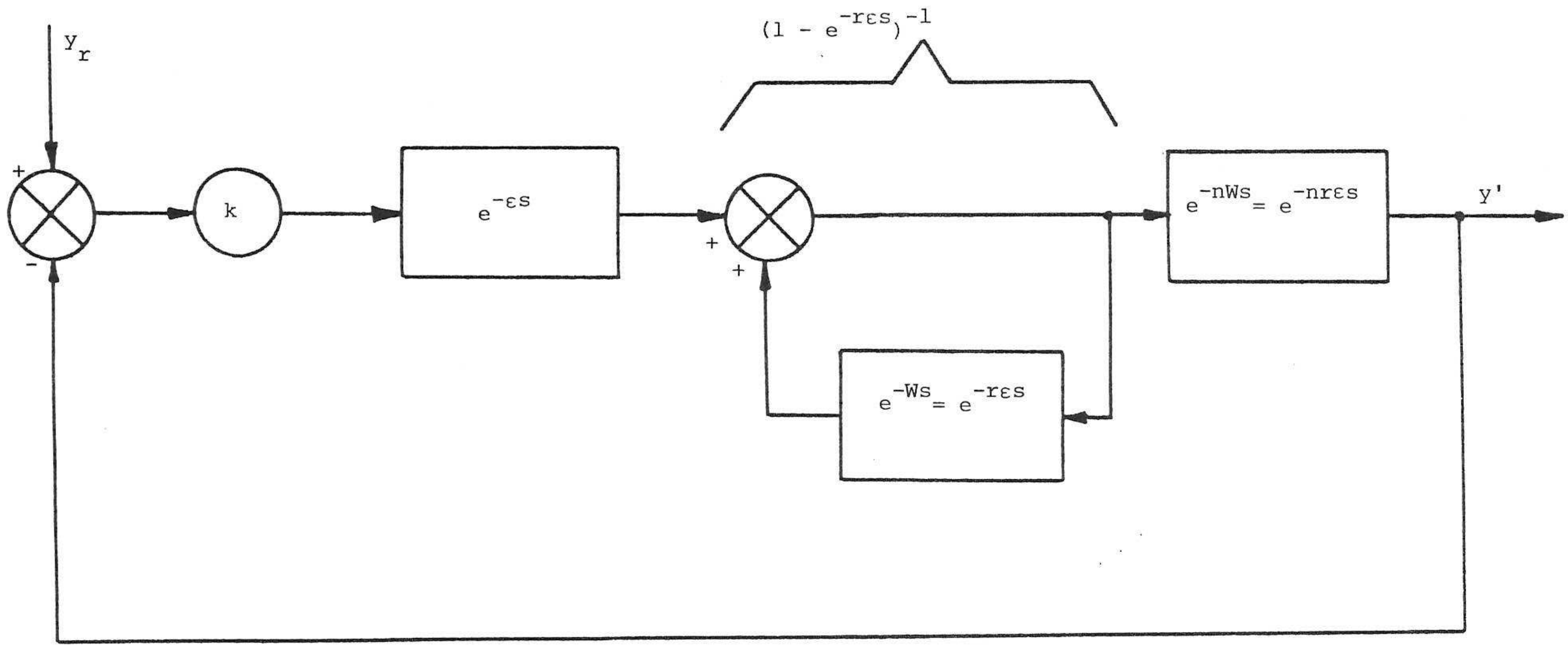

Fig. 5 Block-diagram for dual-delay system having noninteger delay ratio X/W

(i.e. $W = r\,\varepsilon$ and $X = n\,W + \varepsilon$)

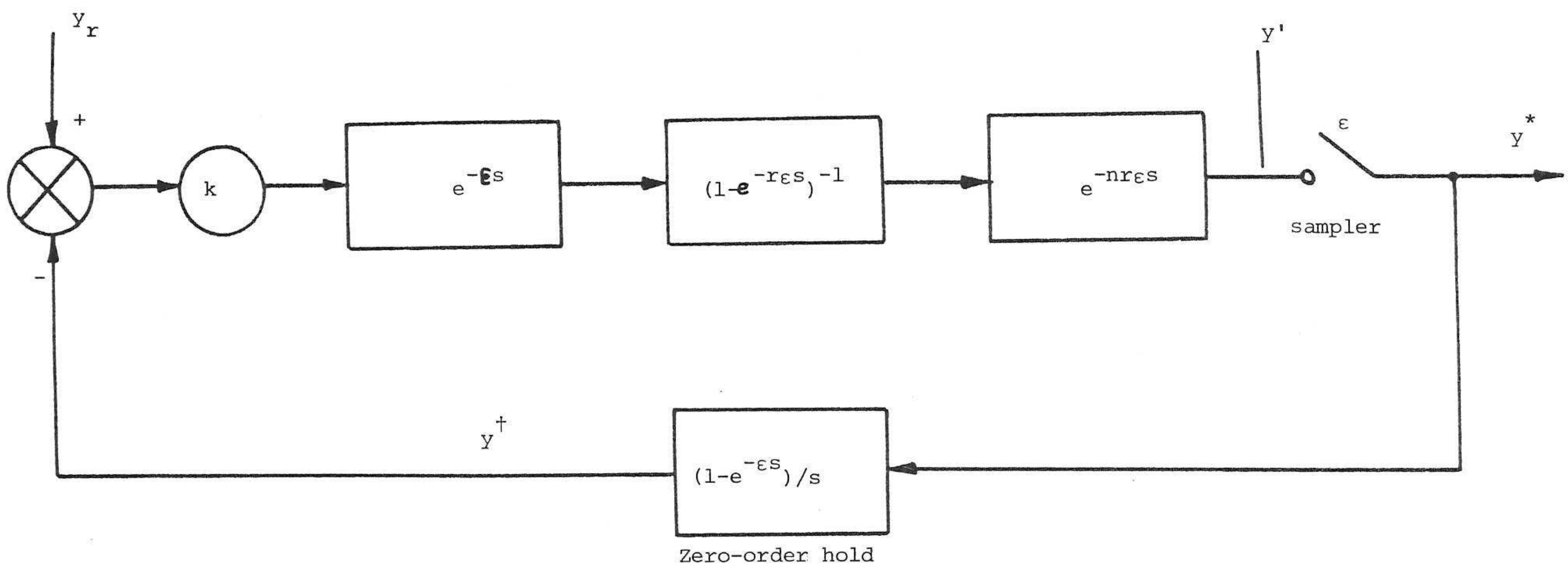

Fig. 6 Block diagram modified for z-transform analysis

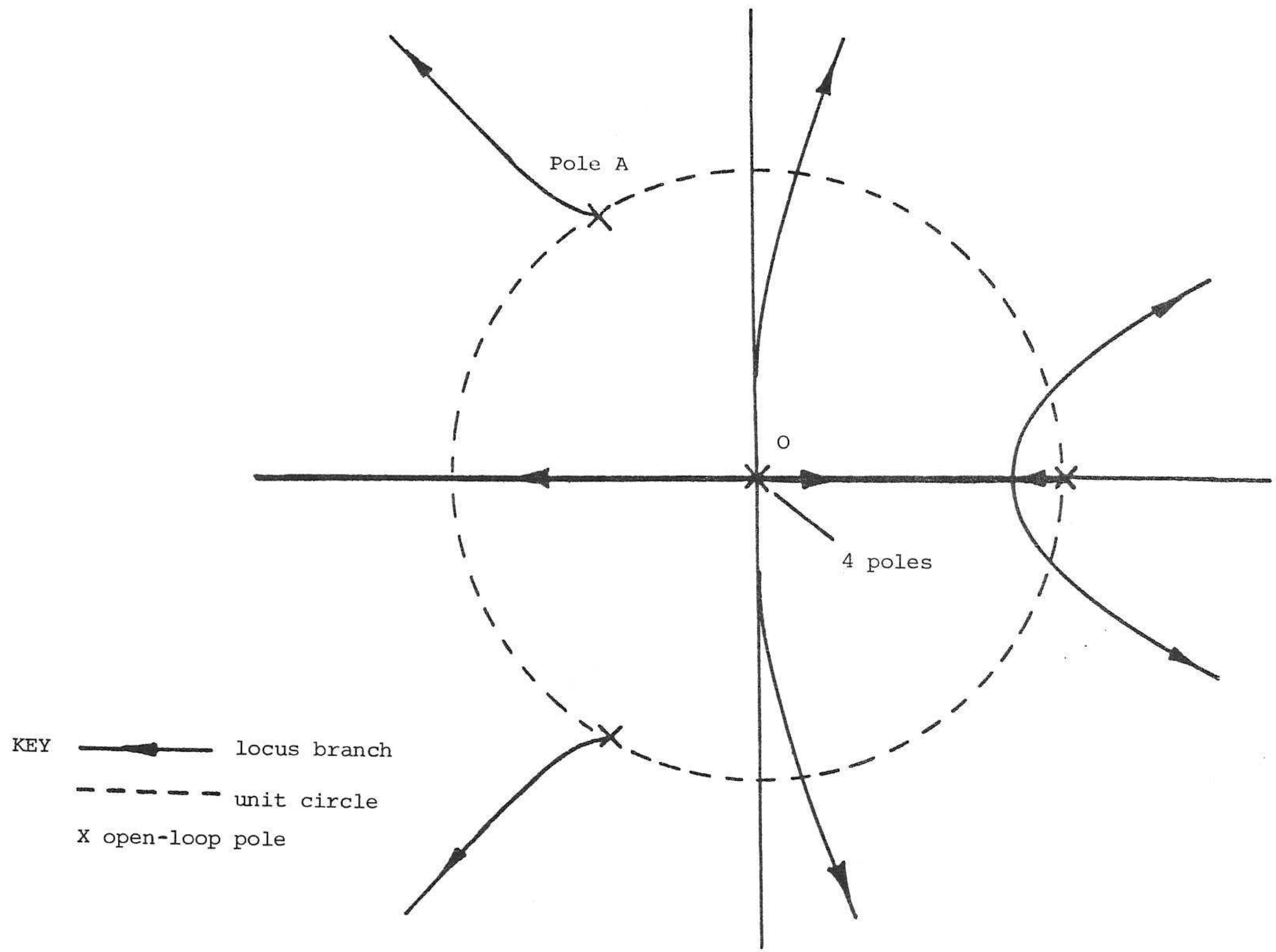

Fig. 7 Root locus for n=2, r=3 (i.e. X = 7W/3)

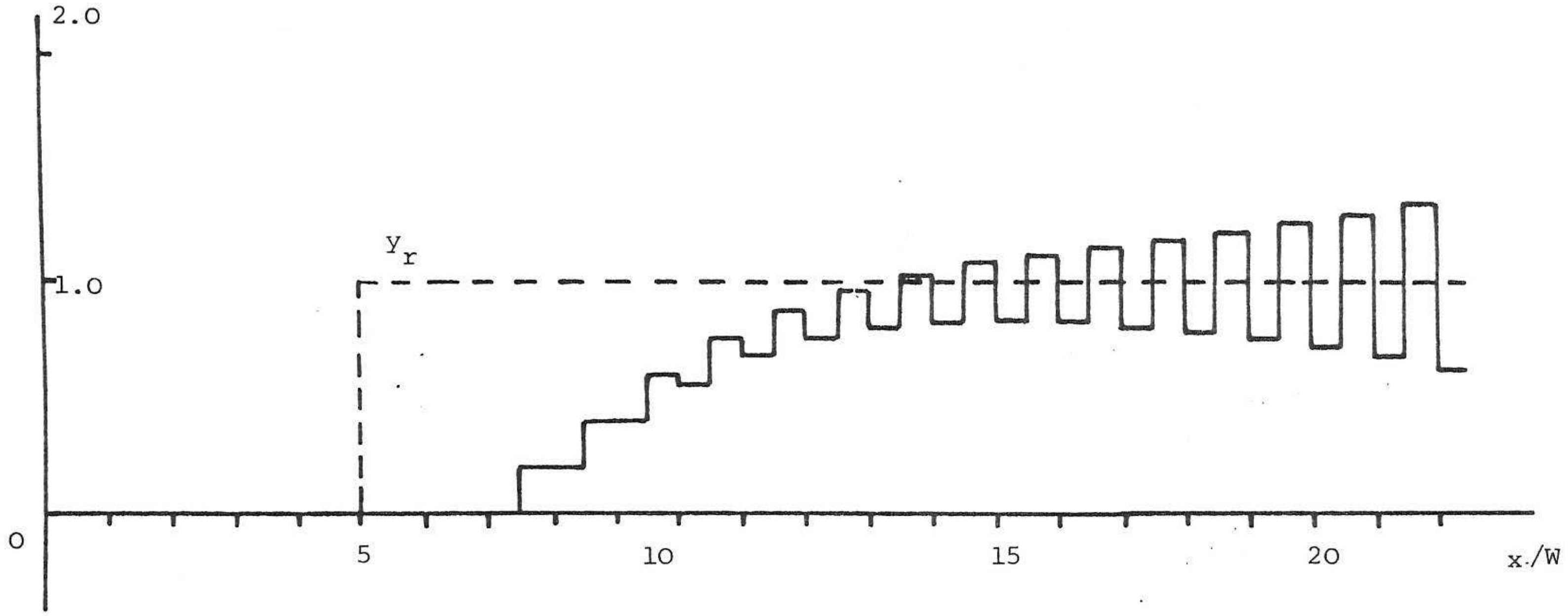

Fig. 8 Unstable unit-step response for n = 2, r = 2 (i.e X = 2.5W), k = 0.0667

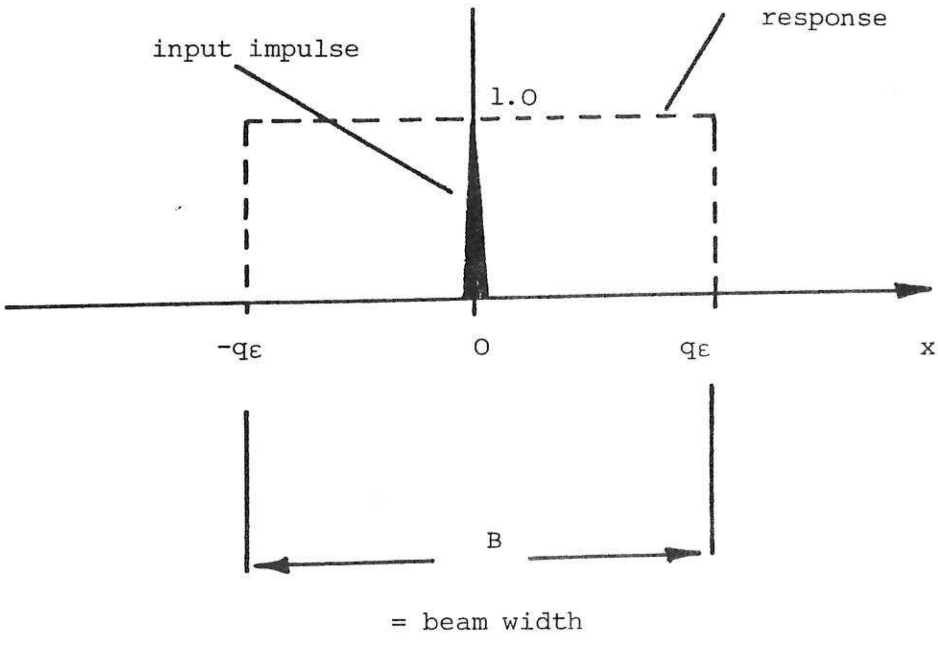

Fig. 9 Impulse Response of Uniform Beam Sensor

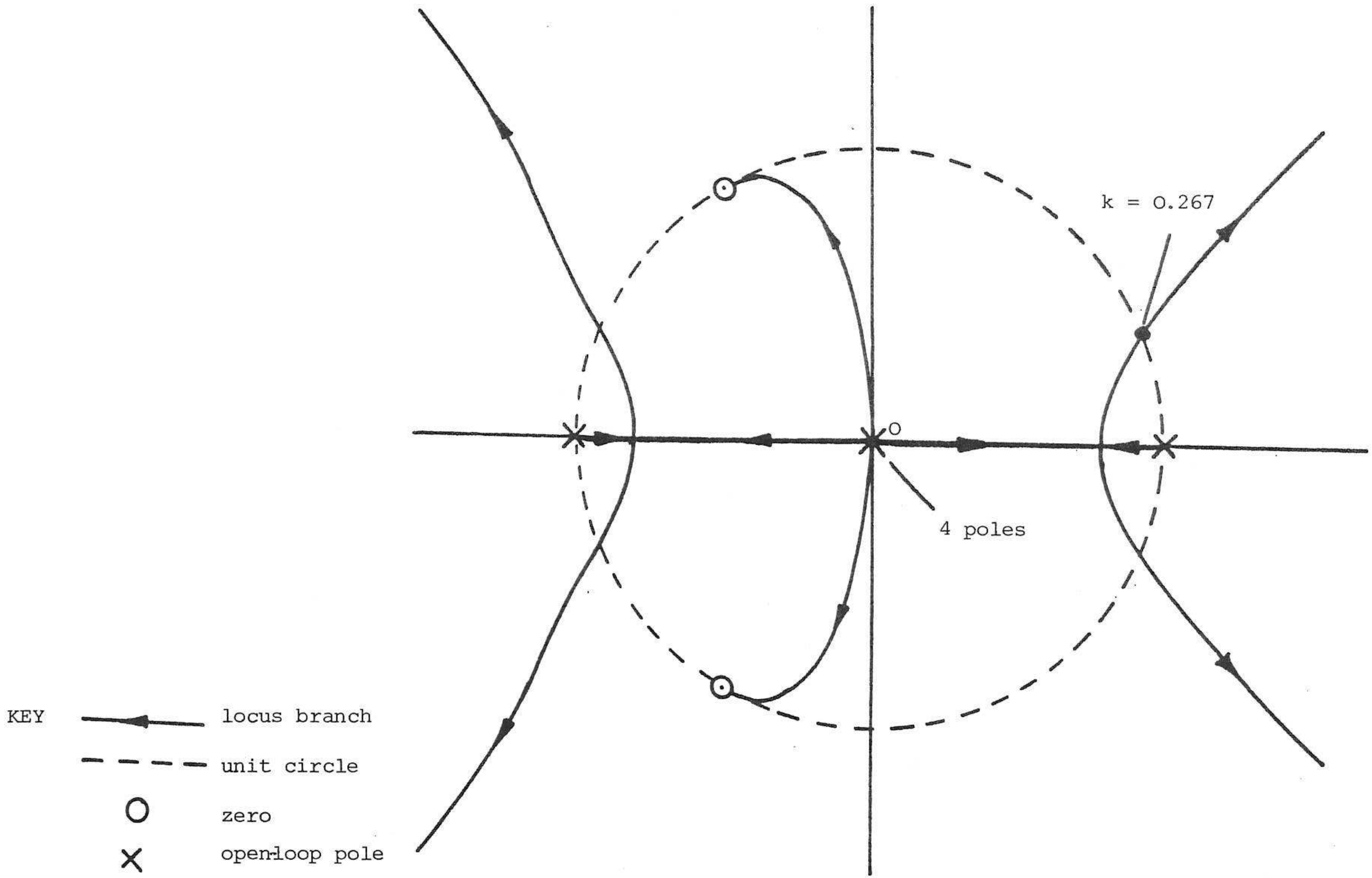

Fig. 10 Root locus for n = 2, r = 2, q = 1, (i.e. X = 2.5W, B = W)

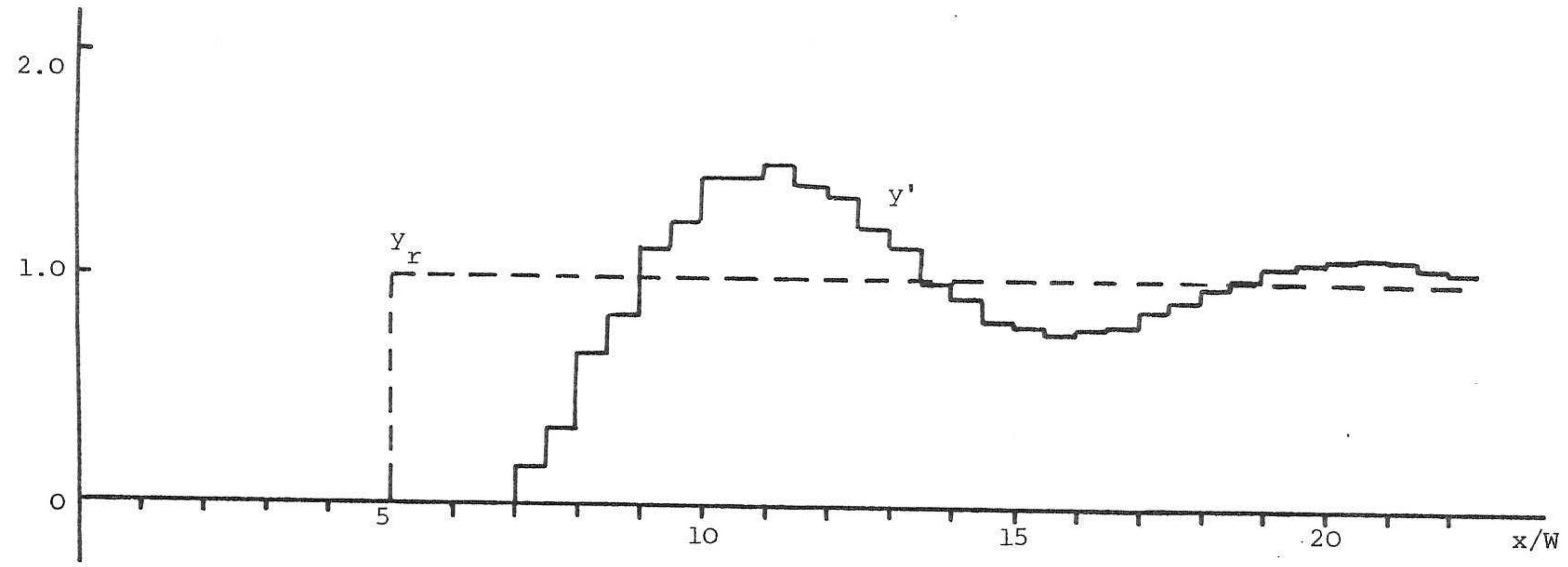

Fig. 11 Unit step-response for n = 2, r = 2, (i.e. X = 2.5W) stabilised by use of sensor with beam-width B = W (k = 0.167)

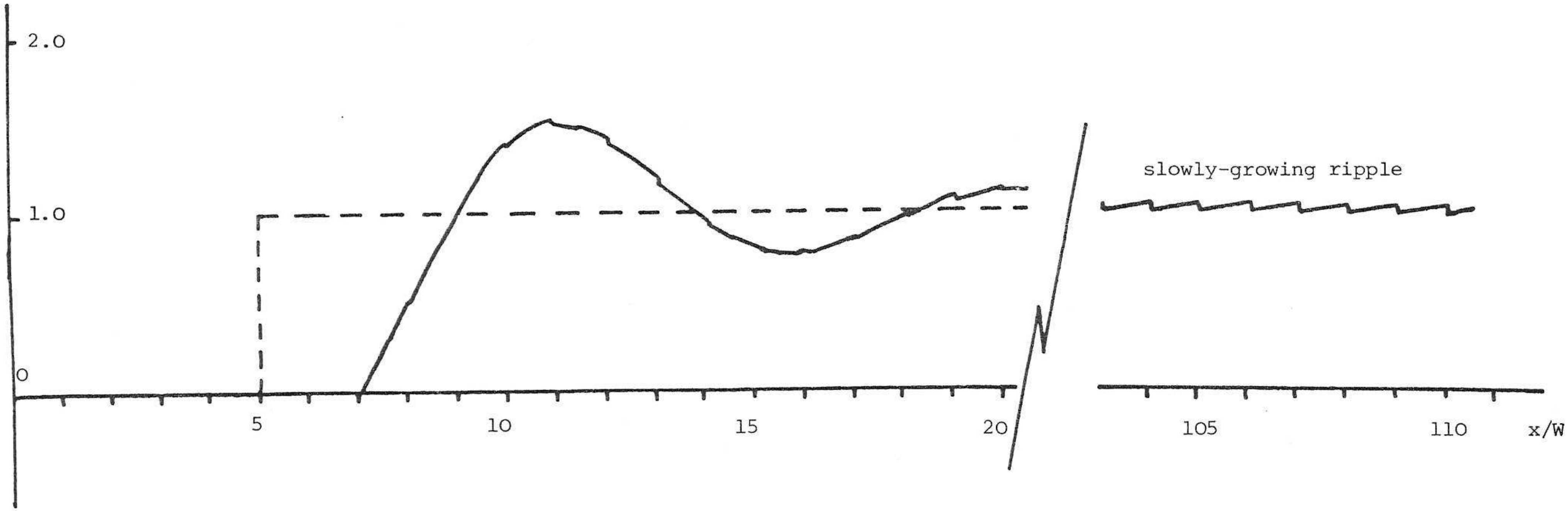

Fig. 12 Unit step response for $n = 2$, $r = 2$ (i.e. $X = 2.5W$) using sensor of beam-width

$B = 0.95\ W$ ($k = 0.167$)